

Numerical Modeling of Disperse Materials Process in a Continuous-Flow Plasma Reactor

B.A. Urmashev* and A. Issakhov

Al-Farabi Kazakh National University, 050040, al-Farabi ave. 71, Almaty, Kazakhstan

Article info

Received:
5 April 2017

Received in revised form:
27 June 2017

Accepted:
18 November 2017

Abstract

The paper presents a numerical simulation of the propagation of the direct-flow temperature plasma reactor, which is solved by the compressible Navier–Stokes equations, numerical algorithm based on SIMPLE algorithm that are approximated by finite volume method. In the numerical solution of the equation system can be divided into four stages. The first stage the transfer of momentum carried out only by convection and diffusion. The intermediate velocity field is solved by the solution of the differential velocity gradient equation, the Green-Gauss Cell Based scheme is used. The second stage for the pressure field, PRESTO numerical scheme is applied. In the third step it is assumed that the transfer is carried out only by the pressure gradient. The fourth step of the equation is solved for the temperature transport equation as well as the momentum equations by the Green-Gauss Cell Based scheme is used. The algorithm is parallelized on high-performance systems. With this numerical algorithm numerical results of temperature distribution in a continuous-flow plasma reactor was obtained. Numerical modeling allows us to give a more precise description of the processes that have been identified or studied theoretically by laboratory methods, and can reveal new physical phenomena processes that are not yet available, seen in experimental studies. Simulation results show that the constructed numerical model provides the necessary accuracy and stability, which should accurately describe the process during the time interval.

1. Introduction

In modern industry, construction and protective materials receive wide and effective use of some powders consisting of hollow microparticles (hollow powder's). Hollow ceramic powders are used in the manufacture of composite heat and acoustic insulation materials, light construction and cement fillers, buoyancy elements, explosive mixtures, as well as to provide a basis for catalysts pit, adsorbents, filter elements, encapsulating medium, etc. Getting hollow microspheres with a given chemical composition and mechanical properties substantially expand the circle of solved problems in the industry of construction and protective materials.

The relevance of the problem of getting dispersed materials undoubtedly due to their highly diverse applications in industry. Dispersed materials, resulting during solidification of mineral binding materials, create important disperse systems in practical terms. Toughness it is the most of their

valuable property. One of the main applications of highly dispersed materials in the industrial production is to use them as an intermediate phase at producing materials with a high degree of activity. In due time the aerosol dispersed materials technology has played a decisive role in ensuring of increasing of uranium – 235 production – nuclear fuel. The natural uranium of this isotope is very small – about 0.7%. To highlight this precious isotope, uranium is converted into gaseous compound – the uranium hexafluoride. This compound is then repeatedly passed through a diffusion baffle, a kind of sieve. The compound lighter uranium-235 is diffused slightly faster than uranium hexafluoride 238 – only 1.005 times. But this is a tiny advantage can be realized only when the pore size of baffle is much less than length of free path of the molecules of UF_6 , which is of the order of 10^{-8} . Producing of such partition is possible only by pressing and sintering particles having a size of the same order.

*Corresponding author. E-mail: baydaulet.urmashev@mail.ru

Historically, the first dispersed product, which was obtained by spray, was soot. There are three types of soot: canal, thermal and heating. Canal soot is obtained by incomplete combustion of natural gas in a channel of rectangular cross section, with walls, which then collected them. Thermal soot is obtained not by combustion, but by the decomposition of natural gas by passing it through the heated by outside channel. This method gives the largest soot particles up to 10^{-8} m radius. The largest capacity provides an oven method in which in a special chamber undergoes incomplete combustion of atomized liquid mixture of hydrocarbons. The resulting aerosol is cooled by passing through a special tower and enters into the apparatus for soot deposition. Soot particles are represented as balls with the size of 10^{-9} – 10^{-8} m aggregated into flakes up to 10^{-6} m, containing hundreds or thousands of «primary» balls. Soot is used not only as filler but also as a black pigment [2].

Dispersed systems – the heterogeneous systems of two or more phases with a high surface area between them. Typically, one of the phases forms a continuous dispersion medium, which is distributed in the volume dispersed phase (dispersed phase or more) as small crystals, solid amorphous particles, droplets or air bubbles. Dispersed systems may have more complex structure, for example, be a two-phase formation, each phases of which, being continuous, enters the volume of the other phase. Such systems include solids, filled with an extensive system of channels-pores, filled with gas or liquid, some microheterogenous polymer compositions and others. There are cases when the dispersion medium «degenerates» to the subtlest layers (membranes), separating the particles of the dispersed phase [1].

There are many papers [16, 17, 25, 31–36] devoted to the study of gas flow in the plasmatron numerically and experimentally. Thus, the experimental part of the gas flow in a plasmatron is described in papers [16, 17, 25, 32, 33]. And in papers [31, 34, 36], numerical simulation of gas flow in a plasmatron is considered. Whereas in paper [35] a very good review on particle simulation of plasma is given.

2. Mathematical model

In discrete analogues of the transport coefficients on the faces of control volumes are determined by harmonically average value, to allow for intermittent changes in the properties of the medium and

to achieve enough correct conjugation at the phase boundary. In solids the thermophysical properties of the wall material (electrode) with the temperature determining of the heavy particles were used. In order to account the heating of the wall by volumetric radiation it was assumed that the radiation energy is absorbed by the surface layer of the wall of the control volumes and is considered there as a local source of heat. Then this energy is given by conduction deeply into the wall and back – to the gas which is adjacent to the wall. To satisfy the safety of wall there is placed a limit on the calculated temperature that does not exceed the melting point of the wall material. Such approach allows us to consider both thermal processes in solids, plasma and gas, and to apply a uniform method of solving equations in the whole computational domain. On the basis of the work [3] a method for simulation the characteristics of the arc from the «cathode to anode» was developed and a satisfactory agreement with the experimental results of the calculation was gotten. This method is convenient to use and does not require any additional information to define the boundary conditions near the solids and relatively easy allows to take into account the form and material of electrodes. The size and location of the cathode and anode arc bindings, the distribution of current density and temperature in the electrodes and the plasma set in the numerical solution as a result of the self-consistent interaction of the thermal, electromagnetic and gas-dynamic characteristics.

In accordance with this, while calculating atmospheric pressure of the high-current arc, in the first approximation there is a possibility to not penetrate into the complex kinetics near electrode processes and for crosslinking solutions, obtained in the electrodes and the plasma, to carry out a simplified scheme: the electrode-plasma.

Now it is known to many mathematical models describing the interaction of electric arc and gas flow in the plasmatron [4–9]. Investigation of the plasmatron's arc propagation with complex geometry is relevant for determining the formation of turbulence and nonequilibrium phenomena in the generation of the plasma flow.

For the development of a numerical model was considered the following assumptions:

- The particles are moving in one direction about the axis of the plasma stream,
- Uniformity of temperature is performed by the particle volume,
- The radiational heat consumption is taken into account,

- Neglect of radiation transfer from the plasma to a particle,

- There is no evaporation particles.

In the considered thermal problem for the hollow particles the characteristic size of the particle is the wall thickness δ . From the considered assumptions, depending on the radius of the particles, it was found that the radiation heat consumption in the heat exchange with the gas is only 5%.

Reynolds-Averaged Navier-Stokes equations form the basis of the present mathematical model. Application of the Boussinesq approximation leads to the following system of equations, where for turbulence modelling the model $k-\varepsilon$ is chosen [10–15]:

$$\frac{\partial \rho}{\partial t} + \frac{\partial \rho u_j}{\partial x_j} = 0 \quad (1)$$

$$\frac{\partial \rho u_i}{\partial t} + \frac{\partial}{\partial x_j} (\rho u_i u_j) = -\frac{\partial p'}{\partial x_i} + \frac{\partial}{\partial x_j} \left[\mu_{eff} \left(\frac{\partial u_i}{\partial x_j} + \frac{\partial u_j}{\partial x_i} \right) \right] \quad (2)$$

$$\frac{\partial E}{\partial t} + \frac{\partial}{\partial x_j} (u_j E) = \frac{\partial u_j E}{\partial x_j} + \frac{\partial q_j}{\partial x_j} \quad (3)$$

$$p = \rho RT \quad (4)$$

where u_i are the velocity components, E – total energy, x_j are the Cartesian coordinate directions, ρ is the mixture density, μ_t is the turbulent viscosity, μ is the viscosity, k is the turbulent kinetic energy, ε is the dissipation rate, μ_{eff} – effective viscosity, p' – modified pressure. Here $p' = p + \frac{2}{3} \rho k + \frac{2}{3} \mu_{eff} \frac{\partial u_k}{\partial x_k}$

and $\mu_{eff} = \mu + \mu_t$ where $\mu_t = C_\mu \rho \frac{k^2}{\varepsilon}$ – turbulence

viscosity, $P_k = \mu_{eff} \left(\frac{\partial u_i}{\partial x_j} + \frac{\partial u_j}{\partial x_i} \right) - \frac{2}{3} \mu_{eff} \frac{\partial u_k}{\partial x_k} \delta_{ij}$, $q = -k \frac{\partial T}{\partial x_j}$,

$E = \rho \left(e + \frac{u^2}{2} \right)$, $e = c_v T$.

$$\frac{\partial k}{\partial t} + \frac{\partial}{\partial x_j} (u_j k) = \frac{\partial}{\partial x_j} \left[\left(\mu + \frac{\mu_t}{\sigma_k} \right) \frac{\partial k}{\partial x_j} \right] + P_k - \rho \varepsilon + P_{kb} \quad (5)$$

$$\frac{\partial \varepsilon}{\partial t} + \frac{\partial}{\partial x_j} (u_j \varepsilon) = \frac{\partial}{\partial x_j} \left[\left(\mu + \frac{\mu_t}{\sigma_\varepsilon} \right) \frac{\partial \varepsilon}{\partial x_j} \right] + \frac{\varepsilon}{k} (C_{\varepsilon 1} P_k - C_{\varepsilon 2} \rho \varepsilon + C_{\varepsilon 1} P_{\varepsilon b}) \quad (6)$$

P_k – turbulent production due to viscous forces, which is represented as:

$$P_k = \mu_t \left(\frac{\partial u_i}{\partial x_j} + \frac{\partial u_j}{\partial x_i} \right) \frac{\partial u_i}{\partial x_j} - \frac{2}{3} \frac{\partial u_k}{\partial x_k} \left(3 \mu_t \frac{\partial u_k}{\partial x_k} + \rho k \right) \quad (7)$$

P_{kb} , $P_{\varepsilon b}$ – represent the buoyancy forces, where

$P_{kb} = -\frac{\mu_t}{\rho \sigma_p} \rho \beta g_i \frac{\partial T}{\partial x_i}$ and $P_{\varepsilon b} = C_3 \max(0, P_{kb})$. Here β is

the coefficient of thermal expansion, $\sigma_p = 0.9$, $C_{\varepsilon 1}$, $C_{\varepsilon 2}$, σ_k , σ_ε – are constants. For the numerical solution, the SIMPLE numerical algorithm was chosen.

3. Numerical algorithm

For the numerical simulation of the system of Eq. (1) – (7) the SIMPLE (Semi-Implicit Method for Pressure Linked Equations) algorithm is applied. This algorithm was first developed by B. Spalding and S. Patankar [18–30].

The solution of the system of Eq. (1) – (7) using SIMPLE algorithm is described shortly with the following steps:

1. First, the boundary conditions were set.

2. The second step is a computation of velocity gradient. For the solution of the differential velocity gradient equation, the Green-Gauss Cell Based scheme is used.

3. After the second step, the pressure gradient is computed. For the pressure field, PRESTO numerical scheme is applied.

4. In order to calculate the intermediate velocity field the discretized momentum equation is solved via the Second Order Upwind scheme.

5. The fifth step is the computation of the uncorrected face mass fluxes.

6. Production of the pressure correction cell values is done at the sixth step due to the solution of the pressure correction equation.

7. At the seventh step, the pressure field $p^{k+1} = p^k + urf \cdot p'$ was updated, where urf stands for the under-relaxation factor for pressure.

8. After updating the pressure field itself, the boundary pressure corrections p'_b was updated too.

9. At the ninth step the face mass fluxes was corrected as following: $\dot{m}_f^{k+1} = \dot{m}_f^* + \dot{m}'_f$.

10. Correction of the cell velocities is done via the solution of next equation: $\vec{v}^{k+1} = \vec{v}^* - \frac{Vol \nabla p'}{\vec{a}_p}$.

11. At the eleventh step, the Volume fraction equation is solved via the CICSAM scheme.

12. The turbulent kinetic energy is solved via the Second order upwind numerical scheme.

13. The thirteenth step is the solution of the Dissipation rate equation, which is done with the application of the Second order upwind scheme.

14. At last step, density and viscosity are updated due to pressure changes.

4. Formulation of the problem

Figure 1 shows a schematic representation of the plasmatron. This figure also indicates all dimensions of the plasmatron. To start simulations, initial and boundary conditions were given. Initial conditions for velocity, pressure, density and temperature are given in the following form: $u_j = 0$, ($j = 1, 2, 3$), $T = 20\text{ }^\circ\text{C}$, $\rho = 1.25\text{ kg/m}^3$, $P = 1\text{ atm}$. The boundary conditions for velocity, pressure, density and temperature are specified, as indicated in Fig. 2. Also, additional boundary conditions are

set for the temperature, depending on the size and location of the heat source. At the lateral boundaries, the non-slip conditions are set for the velocity (Fig. 2).

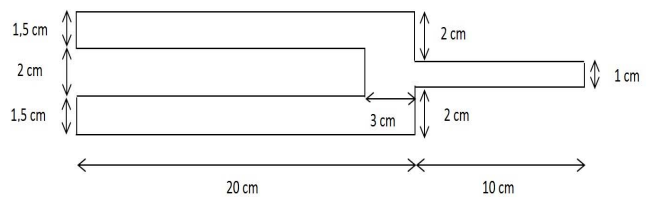


Fig. 1. Schematic view of plasmatron.

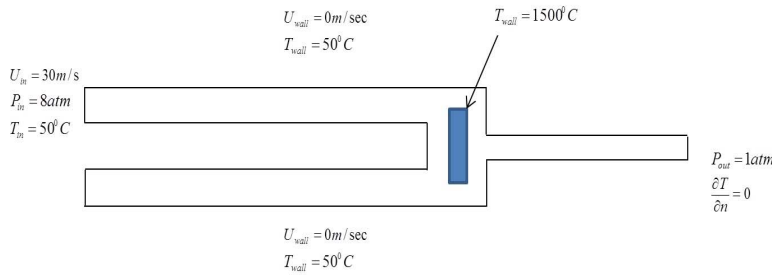


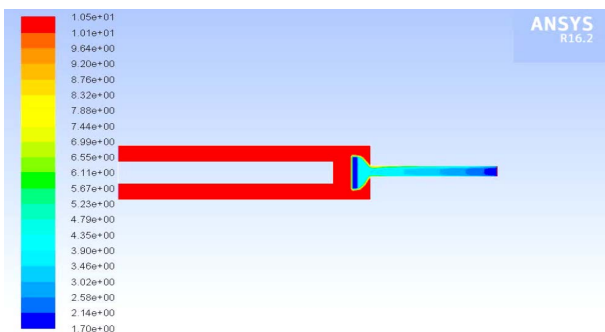
Fig. 2. Boundary conditions.

5. Numerical simulation results

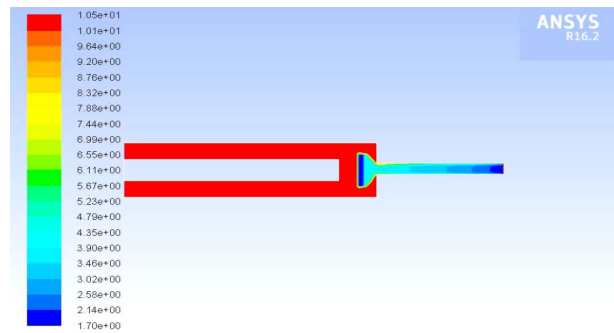
For the numerical simulation, the corresponding initial and boundary conditions were given. The simulations used a computational grid with more than 300 000 computational nodes. To simulate this problem main domain was divided to six subdomains and unstructured mesh was used. To study the temperature distribution, in a direct flow plasma reactor mathematical models were selected and numerical algorithms were developed.

Figure 3 shows the density distribution contour for different time layers in a direct-flow plasma reactor. And in Fig. 4, the contour of Mach number distribution is shown for different time layers in a direct-flow plasma reactor. In Fig. 5, one can see the velocity distribution contour for different time layers in a direct-flow plasma reactor. And in Fig.

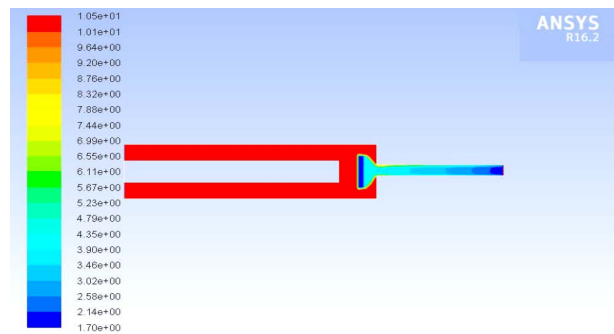
6, the pressure distribution contour is shown for different time layers in a direct-flow plasma reactor. While Fig. 7 shows the temperature distribution profile for different time layers in a direct-flow plasma reactor.



(a)

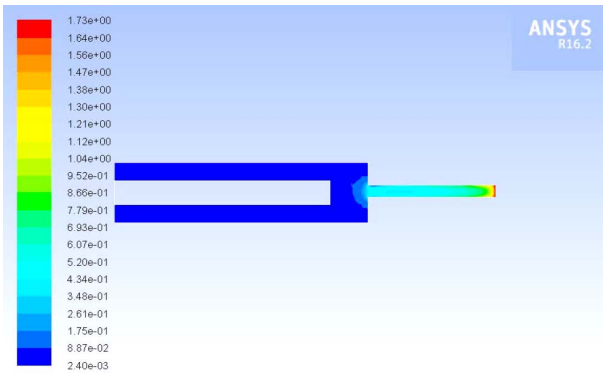


(b)

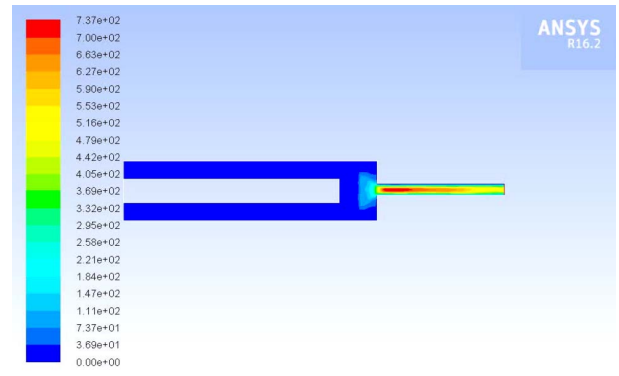


(c)

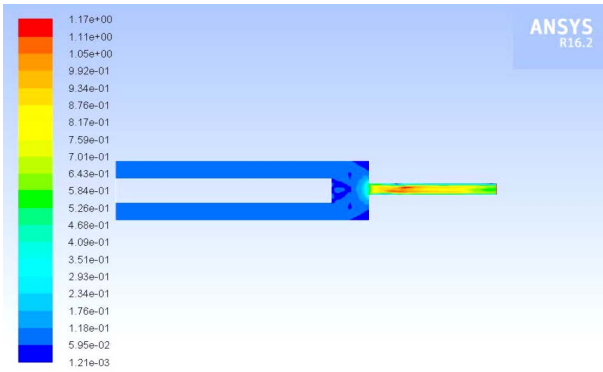
Fig. 3. The density distribution contour for different time layers: (a) $t = 1\text{ sec}$; (b) $t = 15\text{ sec}$; (c) $t = 30\text{ sec}$ in a direct-flow plasma reactor.



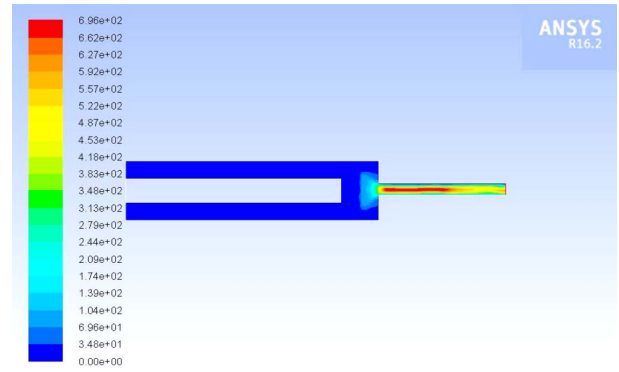
(a)



(b)

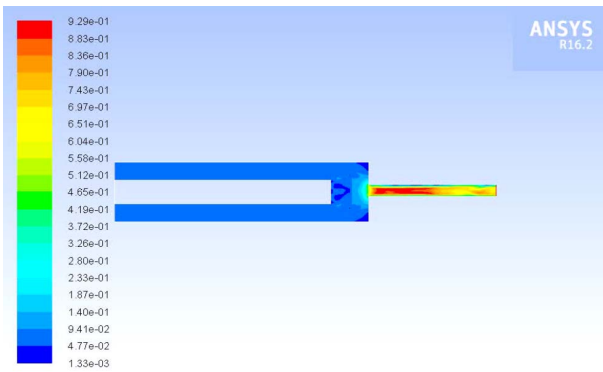


(b)



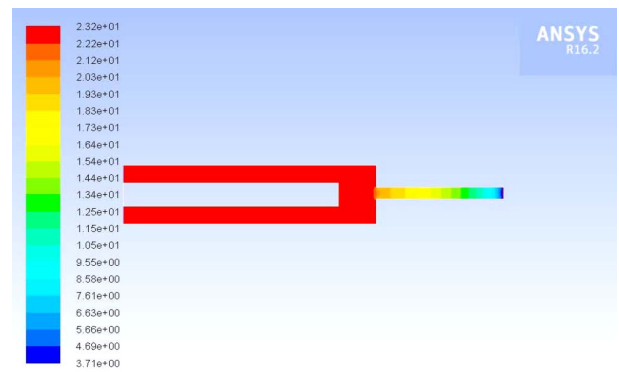
(c)

Fig. 5. The velocity distribution contour for different time layers: (a) $t = 1$ sec; (b) $t = 15$ sec; (c) $t = 30$ sec in a direct-flow plasma reactor.

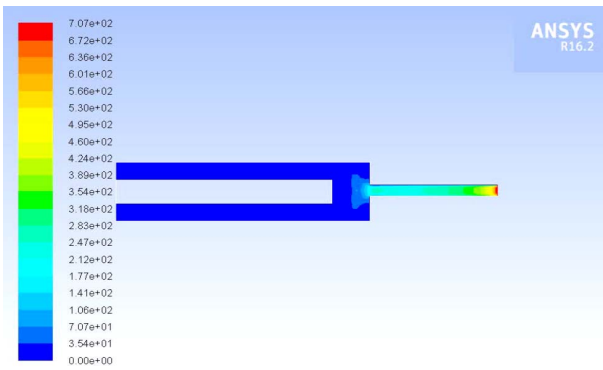


(c)

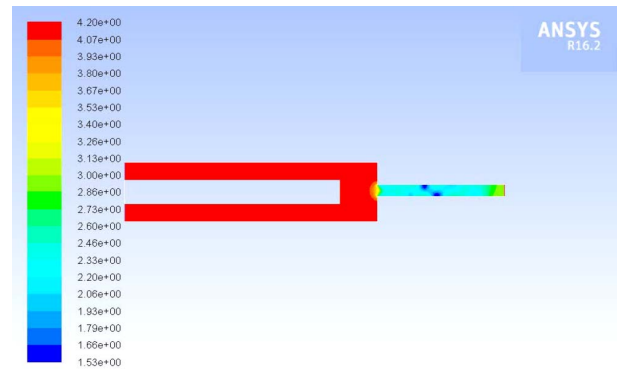
Fig. 4. The Mach number distribution contour for different time layers: (a) $t = 1$ sec; (b) $t = 15$ sec; (c) $t = 30$ sec in a direct-flow plasma reactor.



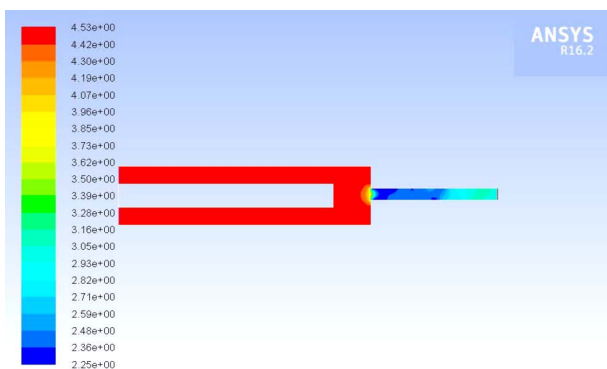
(a)



(a)

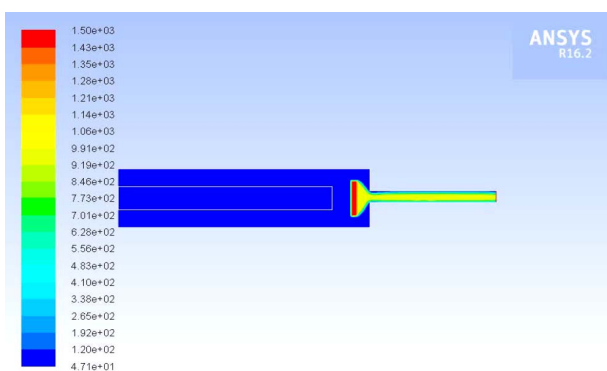


(b)

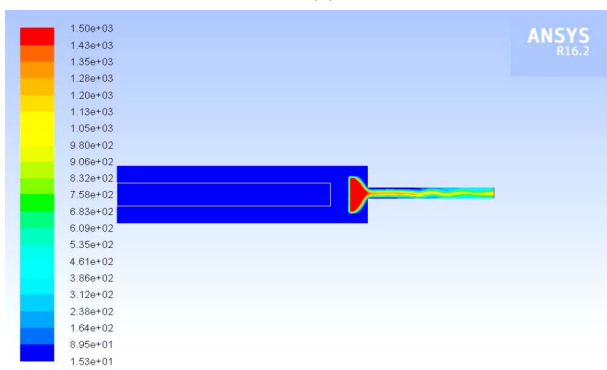


(c)

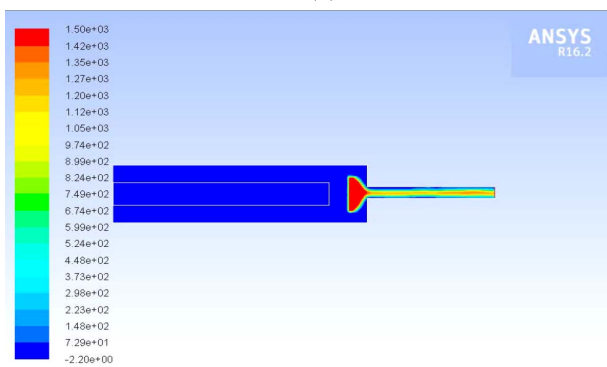
Fig. 6. The pressure distribution contour for different time layers: (a) $t = 1$ sec; (b) $t = 15$ sec; (c) $t = 30$ sec in a direct-flow plasma reactor.



(a)



(b)



(c)

Fig. 7. The temperature distribution contour for different time layers: (a) $t = 1$ sec; (b) $t = 15$ sec; (c) $t = 30$ sec in a direct-flow plasma reactor.

6. Conclusions

In the work numerical modeling of the thermal processes distribution in the direct flow plasma reactor were carried out. This gave a deeper understanding of inner flow in direct flow plasma reactor. Numerical simulation can provide a more accurate description of the technical processes that have been identified or studied theoretically by the laboratory. And also new physical phenomena processes were shown, which not available to see in experimental studies yet.

In the simulation we consider the development of a round jet in a coaxial flow of argon (Ar) at a rate of 29–30 l/min, with the supplied 10–12 gr/min. of ash. For the modeling of a turbulent flow used compressible Navier-Stokes equations consisting of the continuity equation, the momentum equations, the energy equation and equation of state.

Simulation results show that the constructed numerical model provides the necessary accuracy and stability, which should accurately describe the process during the time interval. Here the solution is limited by time, space and the possible range of other physical parameters. It has been found that setting of the boundary conditions is an important task.

Acknowledgements

This work is supported by the grants (0770/GF4 and 2017/GF4) from the Ministry of Education and Science of the Republic of Kazakhstan.

References

- [1]. V.A. Rabinovich. Disperse systems. Encyclopedia of Chemistry, 1985. 704 p. (in Russian).
- [2]. N.B. Uryev. Highly concentrated disperse systems. M., 1980. 502 p. (in Russian).
- [3]. S. Patankar. The exact methods of solving the problems of heat transfer and the dynamics of liquids. M.: Energiya, 1984. 152 p. (in Russian).
- [4]. B.F. Semenov. A turbulent flow of gas in the channel of the plasmotron with a closed electrode is observed. *Bulletin of the Kirghiz-Russian Slavic University*. 5 (2003) 110 p. (in Russian).
- [5]. B.C. Engel'sht, V.T. Gurovich, G.A. Detyatkov and etc. The stability of the arc of the electric arc. Advocacy: Hauka CO 1 (1990) 376 p. (in Russian).

- [6]. A. Zhajnakov, R.M. Urusov, T.Je. Urusova. Pure analysis of non-electronical electric arcs. Bishkek: Ilim, 2001. 232 p. (in Russian).
- [7]. I.G. Panevin, B.I. Hvecjuk, I.P. Hazarenko and etc. Theory and calculation of near-electrode processes. Novo-cherry: Hauka, SB RAS, 10 (1992) 197 p. (in Russian).
- [8]. M.F. Zhukov, I.M. Zasyppkin, A.H. Tymoshevsky, B.I. Mihajlov, G.A. Desjatkov. Electric arc generators of the thermal plasma. Novocity: Hauka, SB RAS, 17 (1999) 712 p. (in Russian).
- [9]. M.F. Zhukov, A.C. Kopoteev, B.A. Upyukov. A typical dynamo of the plasma. Novosibirsk: Hauka SB RAS, 1975. 298 p. (in Russian).
- [10]. D.C. Wilcox. Turbulence Modeling for CFD, 2nd ed. DCW Industries, 2006, – 522 p.
- [11]. T.H. Shih, W.W. Liou, A. Shabbir, Z. Yang, J. Zhu. *Comput. Fluids* 24 (3) (1995) 227–238. DOI: 10.1016/0045-7930(94)00032-T
- [12]. T. Chung, *Computational Fluid Dynamics*. 978-1-107-42525-5 - *Computational Fluid Dynamics: Second Edition*. Cambridge University Press, 2002 – 1012 p. ISBN 978-0-521-76969-3
- [13]. J.H. Ferziger, M. Peric. *Computational Methods for Fluid Dynamics*. Springer; 3rd edition, 2013, – 426 p.
- [14]. R. Peyret, D.Th. Taylor, *Computational Methods for Fluid Flow*. New York: Berlin: Springer-Verlag. 1983, 358 p.
- [15]. P.J. Roache, *Computational Fluid Dynamics*, Albuquerque, NM: Hermosa Publications. 1972, – 434 p.
- [16]. O.P. Solonenko, I.P. Gulyaev, A.V. Smirnov, *J. Therm. Sci. Tech.-JPN* 6 (2) (2011) 219–234. DOI: 10.1299/jtst.6.219
- [17]. I.P. Gulyaev, *Journal of Physics: Conference Series* 441 (2013) 012033, 2013. DOI: 10.1088/1742-6596/441/1/012033
- [18]. S.V. Patankar, D.B. Spalding, *Int. J. Heat Mass Transfer* 15 (10) (1972) 1787–1806. DOI: 10.1016/0017-9310(72)90054-3
- [19]. A. Issakhov, *The Scientific World Journal* 2014 (2014) Article ID 678095, 10 pages. DOI: 10.1155/2014/678095
- [20]. A. Issakhov, *Int. J. Nonlin. Sci. Num.* 15 (2) 115–120. DOI: 10.1515/ijnsns-2012-0029
- [21]. A. Issakhov, *Int. J. Nonlin. Sci. Num.* 16 (5) (2015) 229–238. DOI: 10.1515/ijnsns-2015-0047
- [22]. A. Issakhov, *Appl. Math. Model.* 40 (2) (2016) 1082–1096. DOI: 10.1016/j.apm.2015.06.024
- [23]. A. Issakhov, *Mathematical Modelling of the Thermal Process in the Aquatic Environment with Considering the Hydrometeorological Condition at the Reservoir-Cooler by Using Parallel Technologies. Sustaining Power Resources through Energy Optimization and Engineering*, Eds: Vasant, Pandian, and Nikolai Voropai. IGI Global, 2016, pp. 1–494, Chapter 10 (2016) 227–243. DOI: 10.4018/978-1-4666-9755-3.ch010
- [24]. A. Issakhov, *AIP Conference Proceedings* 1738 (2016) 480025. DOI: 10.1063/1.4952261
- [25]. O.P. Solonenko, Y. Ando, H. Nishiyama, D. Kindole, A.V. Smirnov, A.A. Golovin, S. Uehara, T. Nakajima. Post-treatment of TiO₂ surface layers by quasi-laminar argon-helium plasma jet. In *Proceedings of XIII International conference “Gas-discharge Plasma and Its Application”*. September 5-7, 2017, ITAM SB RAS, Novosibirsk, Russia, 2017. – P. 25.
- [26]. A. Issakhov, *Power, Control and Optimization*. Part of the Lecture Notes in Electrical Engineering book series (LNEE, volume 239). 239 (2013) 165–179. DOI: 10.1007/978-3-319-00206-4_11
- [27]. A. Issakhov, *AIP Conference Proceedings* 1863 (2017) 560050. DOI: 10.1063/1.4992733
- [28]. A. Issakhov, *AIP Conference Proceedings* 1499 (2012) 15–18 DOI: 10.1063/1.4768963
- [29]. A. Issakhov, *Int. J. Nonlin. Sci. Num.* 18(6) (2017) 469–483. DOI: 10.1515/ijnsns-2016-0011
- [30]. A. Issakhov, *International Journal of Energy for a Clean Environment* 16 (2015) 23–28. DOI: 10.1615/InterJEnerCleanEnv.2016015438
- [31]. H.C. Kim, F. Iza, S.S. Yang, M. Radmilovic-Radjenov, and J.K. Lee, *Journal of Physics D: Applied Physics* 38 (2005) R283–R301. DOI: 10.1088/0022-3727/38/19/R01
- [32]. K. Kutasi and Z. Donkó, *Journal of Physics D: Applied Physics* 33 (2000) 1081–1089. DOI: 10.1088/0022-3727/33/9/307
- [33]. M.R. Poor and C. B. Fleddermann, *J. Appl. Phys.* 70(6)(1991)3385–3387. DOI: 10.1063/1.349281
- [34]. H. Ueda, Y. Omura, H. Matsumoto, and T. Okuzawa, *Comput. Phys. Commun.* 79 (1994) 249–259. DOI: 10.1016/0010-4655(94)90071-X
- [35]. J.P. Verboncoeur, *Plasma Phys. Contr. F.* 47 (2005) A231–A260. DOI: 10.1088/0741-3335/47/5A/017
- [36]. D.R. Welch, C.L. Olson, and T.W.L. Sanford. *Phys. Plasmas* 1 (3) (1994) 764–773. DOI: 10.1063/1.870768